A novel toxic effect of foodborne trichothecenes: The exacerbation of genotoxicity

Marion Garofalo, Delphine Payros, Marie Penary, Eric Oswald, Jean-Philippe Nougayrède, Isabelle Oswald

▶ **To cite this version:**

Marion Garofalo, Delphine Payros, Marie Penary, Eric Oswald, Jean-Philippe Nougayrède, et al.. A novel toxic effect of foodborne trichothecenes: The exacerbation of genotoxicity. Environmental Pollution, 2023, 317, pp.120625. 10.1016/j.envpol.2022.120625 . hal-03885045

HAL Id: hal-03885045
https://hal.inrae.fr/hal-03885045

Submitted on 1 Jun 2023

HAL is a multi-disciplinary open access archive for the deposit and dissemination of scientific research documents, whether they are published or not. The documents may come from teaching and research institutions in France or abroad, or from public or private research centers.

L'archive ouverte pluridisciplinaire **HAL**, est destinée au dépôt et à la diffusion de documents scientifiques de niveau recherche, publiés ou non, émanant des établissements d'enseignement et de recherche français ou étrangers, des laboratoires publics ou privés.

Copyright

Manuscript File Click here to view linked References

A novel toxic effect of foodborne trichothecenes: the exacerbation of genotoxicity

Marion Garofalo[a,b], Delphine Payros[a,b], Marie Penary[b], Eric Oswald[b,c], Jean-Philippe Nougayrède[b,T], Isabelle P. Oswald[a,T*].

[a]Toxalim (Research Centre in Food Toxicology), Université de Toulouse, INRAE, ENVT, INP-Purpan, UPS, Toulouse, France

[b]IRSD, Université de Toulouse, INSERM, INRAE, ENVT, UPS, Toulouse, France

[c]CHU Toulouse, Hôpital Purpan, Service de Bactériologie-Hygiène, Toulouse, France

[T]Co senior author

*Corresponding authors: isabelle.oswald@inrae.fr;

Keywords: trichothecenes; genotoxins; colibactin; DNA damage.

ABSTRACT

Trichothecenes (TCTs) are very common mycotoxins. While the effects of DON, the most prevalent TCT, have been extensively studied, less is known about the effect of other TCTs. DON has ribotoxic, pro-inflammatory, and cytotoxic potential and induces multiple toxic effects in humans and animals. Although DON is not genotoxic by itself, it has recently been shown that this toxin exacerbates the genotoxicity induced by model or bacterial genotoxins. Here, we show that five TCTs, namely T-2 toxin (T-2), diacetoxyscirpenol (DAS), nivalenol (NIV), fusarenon-X (FX), and the newly discovered NX toxin, also exacerbated the DNA damage inflicted by various genotoxins. The exacerbation was dose dependent and observed with phleomycin, a model genotoxin, captan, a pesticide with genotoxic potential, and colibactin, a bacterial genotoxin produced by the intestinal microbiota. For this newly described effect, the TCTs ranked in the following order: T-2>DAS>FX>NIV≥DON≥NX. The genotoxic exacerbating effect of TCTs correlated with their ribotoxic potential, as measured by inhibition of protein synthesis. In conclusion, our data demonstrate that TCTs, which are not genotoxic by themselves, exacerbate DNA damage induced by various genotoxins. Therefore, foodborne TCTs could enhance the carcinogenic potential of genotoxins present in the diet or produced by intestinal bacteria.

KEY WORDS

mycotoxins, pesticides, microbiota, colibactin, carcinogenic potential

INTRODUCTION

Mycotoxins are the most prevalent natural dietary toxins and contaminate up to 70% of global crop production (Eskola *et al*., 2020). They represent a major issue for food safety (Payros *et al*., 2021a). These secondary metabolites produced by microscopic fungi are resistant to industrial processes and cooking and contaminate finished processed food. Trichothecenes (TCTs) are one of the most prevalent classes of mycotoxins, comprising over 200 structurally related compounds with a common sesquiterpenoid skeleton (Polak-Śliwińska *et al*., 2021). The differences in their substitution patterns allow TCTs to be classified into four subgroups. Type A TCTs (TCTs-A) and type B TCTs (TCTs-B) are major food contaminants whereas type C and D TCTs rarely occur in food matrices. Type D TCTs have attracted more attention as indoor pollutants (Gottschalk *et al*., 2008). TCTs-A include T-2 toxin (T-2), diacetoxyscirpenol (DAS), and the newly discovered form NX (Varga *et al.*, 2015; Pierron *et al.,* 2022). TCTs-B, which are distinguished from TCTs-A by the presence of a ketonic oxygen at C-8, are mainly represented by deoxynivalenol (DON), nivalenol (NIV) or fusarenon-X (FX) (Figure 1). In Europe, almost 50% of cereals are contaminated with DON (Knutsen *et al*., 2017a), 16% with NIV (Knutsen *et al*., 2017b), and 10% with FX (Schothorst *et al*., 2003). T-2 was detected in 20% of European cereal samples (Knutsen *et al*., 2017c) and DAS in 1.5% of European cereals and cereal-based food (Knutsen *et al*., 2018).

The toxicity of DON, the most prevalent foodborne TCT, is well documented. Acute DON poisoning causes vomiting, nausea, and diarrhoea, while chronic exposure results in food refusal, anorexia, reduced body weight gain, and altered immune responses (Terciolo *et al*., 2018; Pinton and Oswald, 2014; Payros *et al*. 2016). At the cellular level, DON triggers ribotoxicity signalled by protein translation arrest and recruitment of MAP kinases, resulting in inflammation, cytotoxicity and apoptosis, depending on the dose and duration of exposure (Payros *et al.*, 2016; Alassane-Kpembi *et al.*, 2013; Payros *et al*., 2021b). By contrast, other TCTs are largely overlooked in toxicology studies (Seeboth *et al.,* 2010; Alassane-Kpembi *et al*., 2017a; Alassane-Kpembi *et al*., 2017b; Pierron *et al.,* 2022). Additional studies are needed, both because these TCTs are widely distributed in food, and because they induce not only effects similar to DON, such as ribotoxicity, cytotoxicity, inflammation, vomiting and food refusal, but also specific effects. For example, T-2 induces a potent oral irritation effect with skin blistering (Wyatt *et al*., 1973), FX exhibits potent antiviral properties (Tani *et al*., 1995), DAS induces intestinal cell hyperplasia (Weaver, 1981), NIV triggers murine dendritic cells

necrosis not documented for other TCTs (Luongo *et al*., 2010) and NX specifically targets the mitochondria (Soler *et al.,* 2022). The differences between TCTs are also at the molecular level, with differences in the translation step inhibited. Although all TCTs are thought to inhibit peptide elongation (Foroud *et al*., 2019), T-2, DAS, NIV, and FX also inhibit the initiation step, and DON and FX also inhibit translation termination (Cundliffe *et al*., 1977).

DON, which is not genotoxic on its own, has recently been described as capable of increasing the genotoxicity induced by model or bacterial genotoxins (Payros *et al*., 2017, Garofalo *et al*., 2022). This effect is observed with genotoxins with different modes of action, and a role for ribotoxicity has been proposed (Garofalo *et al*., 2022). In this work, we show that the genotoxicity exacerbation is not only an effect of DON, but also of T-2, DAS, NIV, FX, and NX. Importantly, TCTs do not only exacerbate the genotoxicity induced by a model genotoxin, but also the genotoxicity induced by captan, a pesticide contaminating the food, and the genotoxicity induced by colibactin, a genotoxin produced by *Escherichia coli* bacteria in the gut. Thus, although TCTs are not genotoxic, they could enhance the carcinogenic potential of genotoxins present in the diet or in our microbiota.

METHODS

Toxins and reagents. DON, NIV, T-2, FX, and DAS were purchased from Sigma-Aldrich (Saint-Quentin Fallavier, France) and Captan by Dr. Ehrenstorfer (GmbH, Germany/CIL-Cluzeau). Phleomycin (PHM) (13.78 mM) was purchased from Invivogen (Toulouse, France). NX, obtained following the methods described by Aitken *et al*., was a generous gift from D. J. Miller (Aitken *et al.*, 2019). Stock solutions were stored at -20°C. DON (5 mM), NIV (30 mM), T-2 (5 mM), FX (10 mM), DAS (3mM), and captan (50 mM) were dissolved in DMSO; NX (5mM) was dissolved in water.

Cell treatments. Non-transformed rat intestinal epithelial cells (IEC-6, ATCC CRL-1592) were cultured in complete DMEM medium supplemented with 10% foetal calf serum, 1% non-essential amino acids (Fisher scientific, Hampton, USA), and 0.1 U/mL bovine insulin (Sigma-Aldrich), at 37°C with 5% CO_2. The cells were split regularly to maintain exponential growth. A fresh culture was started from a liquid nitrogen stock every 30 passages. The cells were confirmed free of mycoplasma contamination by 16S PCR. For viability assay, cells were seeded in white 96 well plates (Dutscher, Bruxelles, Belgium) and grown to reach ~80% confluence. Cells were then treated for 24 h with various doses of TCTs (or DMSO vehicle) before viability was measured. For ribotoxicity and genotoxicity measurement, cells were

seeded in black 96 well plates (Greiner bio-one, Les Ulis, France) and grown to reach ~80% confluence. For ribotoxicity measurement, cells were incubated for 4 h with various doses of TCTs or DMSO vehicle followed by a 30 min incubation with puromycin (Sigma-Aldrich) at a final concentration of 10 µg/mL. For PHM and captan-induced genotoxicity measurement, cells were co-treated for 4 h with 5 µM PHM or 10 µM of captan and various doses of TCTs.

Preparation of colibactin-producing bacteria. The intestinal carcinogenic *Escherichia coli* strain NC101 that produces the genotoxin colibactin, and the isogenic mutant strain NC101Δ*clbP* which do not produce the toxin (Yang *et al*., 2020) were cultured in Lysogeny-broth (LB) Lennox medium overnight at 37°C with shaking. Epithelial cell-bacteria interaction medium DMEM 25 mM Hepes (Fisher scientific) was inoculated from overnight bacterial cultures and incubated at 37°C with shaking until the bacteria reached an optical density at 600 nm of 0.5 before infection.

Colibactin-induced genotoxicity measurement. IEC-6 cells were infected with *E. coli* producing colibactin as described previously (Payros *et al.*, 2017). Briefly, cells were incubated with different doses of TCTs and infected for 4 h with wild type (WT) *E. coli* NC101 or the *clbP* isogenic mutant. Cells were then washed and incubated in complete DMEM medium supplemented with 200 µg/mL gentamicin and maintained 4 h post-infection in the presence of TCTs or DMSO vehicle, and then fixed for DNA damage measurement.

Viability assay. Cell viability was assayed with the CellTiter-Glo Luminescent Cell Viability Assay (Promega, Charbonnières-les-Bains, France) as described (Khoshal *et al.,* 2019). Luminescence was measured with a spectrophotometer (TECAN Spark, Mannedorf, Switzerland).

Ribotoxicity analysis by In-Cell-Western. Ribotoxicity was measured using protein synthesis inhibition as a surrogate. The measurement of protein synthesis by puromycin labelling was performed as described (Henrich, 2016). Briefly, puromycin was immuno-detected by In-Cell-Western using an anti-puromycin antibody (clone 12D10 diluted 1:5000; Millipore, Molseihm, France). GAPDH, which is constitutively expressed and has a half-life of 8 h (Dani *et al*., 1984), was used as a control. The anti GAPDH antibody was diluted 1:5000 (ABS16; Millipore). Secondary antibodies were diluted 1:5000 (IRDye 800CW; Rockland, and IRDye 680RD Licor). Puromycin signal was normalized with the average fluorescence of puromycin-labelled control cells (Henrich, 2016).

Quantification of DNA damage by In-Cell-Western. In-Cell-Western was performed as previously described (Martin *et al.*, 2013; Tronnet and Oswald, 2018; Theumer *et al.,* 2018). Briefly, fixed cells were permeabilized and stained with the primary antibody anti-γH2AX (20E3 diluted 1:200; Cell Signalling, Saint-Quentin en Yvelines, France). Secondary antibody (IRDye 800CW diluted 1:1000; Rockland) and RedDot2 DNA marker (Biotium) were measured at 680 and 800 nm with a Sapphire Biomolecular Imager (Azure Biosystems). The genotoxic index was calculated by dividing the γH2AX signal by the corresponding DNA fluorescence and normalized with the average signal in control cells (Tronnet and Oswald, 2018).

Data analysis. GraphPad Prism 8.0 was used to calculate concentrations that inhibited the cell viability by 20% (IC_{20}), and the protein synthesis by 20% (20% PSI level), performing a four-parameter nonlinear regression model (sigmoidal dose-response analysis). Profile-likelihood confidence intervals were calculated from the nonlinear regressions. One-way analysis of variance (ANOVA) followed by Bonferroni's multiple comparison were performed. The data are expressed as mean ± SEM.

RESULTS

Trichothecenes induce a dose-dependent reduction in cell viability. As the intestinal tract is the primary target of TCTs, the non-transformed intestinal epithelial cell line IEC-6 was used. Cytotoxicity was first evaluated 4 h and 8 h after TCTs treatment, and no cytotoxicity was detected (Table S1). The effect of TCTs on cell viability was then evaluated 24 h after treatment, and we observed a dose-dependent inhibition of viability induced by DON, NIV, T-2, FX, DAS and NX (Figure 2A). IC_{20} values, which correspond to the dose inducing a 20% reduction of cell viability, were calculated for each TCT (Figure 2B). For cytotoxicity, TCTs were classified as follows: T-2>DAS>FX>NIV>NX>DON.

Trichothecenes induce a dose-dependent ribotoxicity. Ribotoxicity is the main mode of action of TCTs (Pestka, 2010). To quantify the ribotoxicity of the TCTs, we examined translational inhibition, assessed by the incorporation of the protein translation marker puromycin in newly synthesized peptides (Henrich, 2016). The incorporated puromycin was quantified by immunofluorescence. All the TCTs induced a dose-dependent ribotoxicity (Figure 3A). Treatment with TCTs did not induce a drop in GAPDH levels (which has an 8 h

half-life), confirming that puromycin specifically labelled newly synthesized peptides (Figure 3A, Figure S2). The doses inducing a 20% reduction in protein synthesis were calculated (Figure 3B). For their ribotoxic effect, TCTs were classified as follows: T-2>DAS>FX>NIV>NX≥DON.

Trichothecenes exacerbate DNA damage induced by the drug phleomycin. The genotoxic exacerbation properties of TCTs were first evaluated with phleomycin (PHM), a genotoxin commonly used as a model for genotoxicity assessments (Chen and Stubbe, 2005). IEC-6 cells were treated for 4 h with PHM and/or TCTs. As expected, cells treated with PHM alone exhibited DNA damage signalled by the γH2AX marker (Rogakou *et al*., 1998). TCTs alone did not induce γH2AX, indicating that they are not genotoxic by themselves. In contrast, all the TCTs induced exacerbation of PHM-induced DNA damage, in a dose-dependent manner (Figure 4A). A significant increase occurred from 1 μM for DON, 3 μM for NX, 10 nM for T-2, 0.3 μM for FX, 30 nM for DAS, and 3 μM for NX (Figure 4B). The exacerbation of genotoxicity did not induce cell detachment, indicating that this effect was not a consequence of massive cell death (Figure 4, Table S1).

Trichothecenes exacerbate DNA damage induced by captan, a pesticide which contaminates food. We then tested the ability of TCTs to exacerbate genotoxicity induced by a food-contaminating genotoxin, such as the pesticide captan, which can be found in fruits, vegetables, and cereals (Shinde *et al*., 2019). For this purpose, IEC-6 cells were exposed to captan and/or TCTs for 4 h. Captan alone induced DNA damage, and TCTs induced an exacerbation of the genotoxicity of captan, in a dose-dependent manner. Significant increase occurred from 3 μM for DON and NX, 1 nM for T-2, 1 μM for FX, and 3 nM for DAS, and did not induce cell death (Figure 5, Table S1).

Trichothecenes exacerbate genotoxicity induced by colibactin, a genotoxin produced by members of the intestinal microbiota. We then determined whether TCTs also exacerbate genotoxicity induced by a bacterial genotoxin produced by the intestinal microbiota, colibactin. The genotoxicity of colibactin was measured by infecting IEC-6 cells with the live colibactin-producing bacterium *Escherichia coli* NC101. Since colibactin is unstable and is not purifiable, direct contact between live colibactin-producing *E. coli* strain and eukaryotic cells is required to induce DNA damage (Chagneau *et al*., 2022; Nougayrède *et al.*, 2006; Bossuet-Greif *et al.*, 2018). Cells were infected with strain NC101 and either co-treated with TCTs or not. Cells

infected with the WT strain showed an increase in their γH2AX signal, resulting from colibactin damage, whereas cells infected with the NC101 Δ*clbP* strain, which is impaired for colibactin synthesis, did not show DNA damage (Figures 6, S1). By contrast, TCTs-treated and WT-infected cells exhibited exacerbation of colibactin-induced DNA damage, which increased with TCT dosage. A significant increase occurred at 3 µM for DON, NX and NIV, 1 nM for T-2, 0.3 µM for FX, and 10 nM for DAS (Figure 6), and was not associated with cell death (Table S1). Exacerbation of DNA damage was not associated with increased colibactin production by TCT-treated bacteria, nor was it associated with an impact of TCTs on bacterial growth (Supplementary methods 1, Figure S1).

DISCUSSION

Food contamination by TCTs is a public health issue of the utmost importance. TCTs levels in foods are indeed high and may even increase in the future, in part due to climate change (Van Der Fels, 2016). DON, which is not genotoxic, was recently described as a genotoxicity enhancer (Garofalo *et al*., 2022; Payros *et al*., 2017). In this work, we show that this is not only an effect of DON, but also a novel effect attributable to at least five other TCTs: NIV, T-2, FX, DAS and the recently discovered NX toxin. These TCTs exacerbate not only the genotoxicity induced by the model genotoxin phleomycin, but also the genotoxicity induced by captan, a pesticide with genotoxic properties, and by colibactin, a bacterial genotoxin produced in the gut. For this newly identified effect, TCTs were classified as follows: T-2>DAS>FX>NIV≥DON≥NX.

The cytotoxicity of TCTs was compared in non-transformed IEC-6 intestinal cells. Our data show that TCTs, which were not cytotoxic after a treatment lasting 4 h or 8 h, induced a dose-dependent inhibition of cell viability after 24 h. These data allowed the classification of TCTs as follows: T-2>DAS>FX>NIV>NX>DON. Although, to the best of our knowledge, this is the first direct comparison and ranking of TCTs' cytotoxicity in IEC-6 cells, the classification is consistent with the literature. T-2 toxin is indeed known as the most toxic TCT, with IC_{20} about 1000 times greater than others (Fernández-Blanco, 2018). DAS is slightly less cytotoxic than T-2, but more than FX (Moon, 2003), and FX is more cytotoxic than NIV and DON (Aupanun *et al.*, 2019; Alassane-Kpembi *et al.*, 2017a). We observed that IEC-6 cells exhibit a modest sensitivity to DON. As a matter of fact, after 24 h of treatment, we found an IC_{20} of 20.2 µM when others found IC_{20} of ≈0.5 µM in IPEC-1 cells, or ≈3 µM in Caco-2 cells (Alassane-Kpembi *et al*., 2015; Pierron *et al*., 2022). Our results are consistent with those obtained by Bianco *et al*., who found an IC_{50} for DON of 50.2 µM in IEC-6 cells, confirming

the limited sensitivity of this cell line (Bianco *et al*., 2012). In addition, our results highlight that NX is approximately twice as cytotoxic as DON in IEC-6 cells. This result is consistent with the results of Pierron *et al*. which showed a higher inflammatory potential for NX compared to DON in porcine intestinal explants (Pierron *et al*., 2022). In contrast, the literature shows that NX-induced cytotoxicity is comparable to that of DON in HT-29 and Caco-2 cells (Varga *et al*., 2018; Pierron *et al*., 2022). Importantly, the doses of TCTs that were cytotoxic after 24 h of exposure were higher than the doses that exacerbated genotoxicity (Table 1). This indicates that non-cytotoxic doses of TCTs exacerbate genotoxicity. Because DNA damage is a source of genetic mutations through repair errors, this result raises questions about the fate of these cells (Basu, 2018). Cells co-exposed to genotoxins and TCTs survive and could therefore pursue their cell cycle and division following repair of DNA damage. Further studies are needed to examine whether cells co-exposed to TCTs and genotoxins could accumulate mutations, ultimately resulting in cellular transformation.

In this work, we also classified TCTs for their ribotoxicity. The ranking T-2>DAS>FX>NIV>NX≥DON parallels that obtained for cytotoxicity and is coherent with the structures of TCTs. The most ribotoxic TCTs carry substitutions thought to improve binding to the ribosome, such as the isovaleryl group at C_8 in T-2 or the acetyl groups at C_4 and C_{15} in DAS (Wu *et al*., 2013; Wang *et al.*, 2021). Differences in TCTs' ribotoxicity may also be related to divergences in structural rearrangements induced by ribosome binding (Garreau de Loubresse *et al*., 2014). Depending on the structure of TCTs, structural rearrangements could differ and induce variations in the mode of protein synthesis inhibition. We have previously suggested that DON-induced ribotoxicity is involved in the genotoxicity exacerbation phenotype. Indeed, ribotoxic compounds reproduced the effect, while the non-ribotoxic DON derivative DOM-1, did not (Garofalo *et al*., 2022). The correlation between TCTs' ribotoxic and genotoxicity exacerbating doses observed in this work (Table 1) support this hypothesis. Interestingly, TCTs with substitutions that increase affinity to the ribosome have a greater capacity to exacerbate genotoxicity. This suggests that there is a structure-function link between ribotoxicity and genotoxicity exacerbation. TCTs could be classified into 3 subgroups according to their capacity to exacerbate the genotoxicity, with regard to their affinity with the ribosome: T-2, DAS > FX > NIV, NX, DON.

Several mechanism could be involved the ribosome-dependent exacerbation of genotoxicity. In response to DNA damage, cells reprogram their gene expression to synthetize proteins of the DNA damage response (Spriggs, Bushell and Willis, 2010). TCTs-induced ribotoxicity could disrupt the production of these stress response proteins. Through their

ribotoxic effect, TCTs can induce inflammation (Pestka, 2010; Garcia et al 2018), which represses the DNA damage response (Jaiswal *et al.*, 2000). Finally, it has been documented that DON activates the protein kinase R (PKR), which triggers inhibition of the DNA damage repair and sensitizes cells to DNA damage (Zhou *et al.*, 2014). As they share structural similarities with DON, TCTs could also recruit PKR and induce sensitization to DNA damage. Further work is required to understand how ribotoxicity results in this novel effect of TCTs.

We observed that exacerbation of genotoxicity occurred at realistic doses of TCTs. The European Food Safety Authority (EFSA) established a no observable adverse effect level (NOAEL) for DON of 100 µg/kg body weight (bw)/day (Knutsen *et al*. 2017a), and 65 µg/kg bw/day for DAS (Knutsen *et al*., 2018). The Benchmark Dose Limit ($BMDL_{10}$) for NIV is 350 µg/kg bw/day (Knutsen *et al*., 2017b), and 3.3 µg/kg bw/day for T-2 (Knutsen *et al*., 2017c). Estimating, as Maresca *et al*., 2013, that for a human weighing 70 kg, the small intestine content is 1L, these doses can be converted to intestinal concentrations of 23.6 µM DON, 0.5 µM T-2, 12.5 µM DAS, and 78.4 µM NIV. Our study shows no effect doses for genotoxicity exacerbation well below these reference values, with 1 µM, 3 nM, 10 nM, and 3 µM for DON, T-2, DAS and NIV, respectively. We observed that structurally related TCTs displayed comparable effects, and could therefore be classified into 3 subgroups: T-2, DAS > FX > NIV, NX, DON. As TCTs frequently co-occur in foodstuffs (Alassane-Kpembi *et al*., 2017b), it would be appropriate to set group TDIs for TCTs, as it has been done for other groups of structurally related mycotoxins (Steinkellner *et al*. 2019).

The exacerbation effect occurred with captan, a pesticide which induces *in vitro* DNA damage (Fernandez-Vidal *et al*., 2019). Captan can contaminate fruits and vegetables, but also cereals, which are the main source of TCTs (Shinde *et al*., 2019). Captan has been associated with multiple myeloma in farmers (Presutti *et al*., 2016), and is classified by the European Commission as “suspected of causing cancer” (European Commission, 2008). Notably, the exacerbation effect occurred at realistic doses of captan. The NOAEL for captan is indeed 25 mg/kg bw per day (Anastassiadou *et al*., 2020), which corresponds to an intestinal concentration of 5.8 mM. Here, the exacerbated genotoxic effect of captan was observed with a dose as low as 10 µM, well below the NOAEL. Interestingly, TCTs also exacerbate the effect of colibactin, an endogenous genotoxin produced by the intestinal microbiota throughout the host’s life. Indeed, approximately 15% of 3-day-old neonates are colonized by colibactin-producing *E. coli* (Payros *et al*., 2014), and 25% of adults harbour these bacteria (Putze *et al*., 2009; Tenaillon *et al*., 2010; Johnson *et al*., 2008). In addition, the prevalence of the B2 phylogenetic group of *E. coli*, which includes up to 50% of colibactin-producing strains, is increasing in developed

countries (Tenaillon *et al*., 2010). The intestinal microbiome also encodes other bacterial genotoxins such as cytolethal distending toxins (Taieb *et al*., 2016). Thus, humans are potentially co-exposed to TCTs together with endogenous genotoxins produced by the microbiota as well as multiple exogenous diet-borne genotoxins, such as captan, and other genotoxic pesticides such as glyphosate (International Agency for Research on Cancer, 2017), alcohol-derivatives (Brooks *et al*., 2014), and components of red meat (Bastide *et al*., 2011). Given the high prevalence of TCTs in foods, it is conceivable that TCTs could exacerbate the effect of the multiple genotoxic agents to which we are exposed.

CONCLUSION

We report that even though TCTs are not genotoxic by themselves, these contaminants promote the genotoxicity of genotoxins which are in the diet, such as pesticides, or are produced by the intestinal microbiota. Considering the wide prevalence of both TCTs and genotoxins, a large part of the population could be impacted by this novel effect. This is alarming because DNA damage drives cancer development (Basu, 2018). A preliminary report on a large-scale epidemiological study in the European Union has suggested a link between long-term exposure to DON and an increased risk of colon cancer (Huybrechts *et al*., 2019). If confirmed, exacerbation of DNA damage by DON could be a key to explaining this epidemiological link. Here, we show that DON is not the only dietary TCT to exhibit this genotoxicity-exacerbating property. There is an urgent need for additional studies on the impact of TCTs on carcinogenesis induced by other environmental toxicants.

ACKNOWLEDGMENTS

We thank David J. Miller for the gift of NX. We thank Julien Vignard (Toxalim) for the scientific input. We are grateful to Elisha Oliver for editing the language. This work was supported by grants from the French Agence Nationale de la Recherche (Genofood ANR-19-CE34 and GenoMyc ANR-22-CE34). MG was supported by a fellowship from the French ministry for Higher Education and Research.

REFERENCES

Aitken A., Miller J.D. and McMullin D.R. 2019. ‘Isolation, chemical characterization, and hydrolysis of the trichothecene 7α-hydroxy, 15-deacetylcalonectrin (3ANX) from *Fusarium graminearum* DAOMC 242077’, *Tetrahedron Lett.*, 60:852–856. doi:10.1016/j.tetlet.2019.02.025.

Alassane-Kpembi I., Kolf-Clauw M., Gauthier T., Abrami R., Abiola F.A., Oswald I.P., Puel, O. 2013. 'New insights into mycotoxin mixtures: The toxicity of low doses of Type B trichothecenes on intestinal epithelial cells is synergistic', *Toxicol. Appl. Pharmacol.*, 272:191–198. doi:10.1016/j.taap.2013.05.023.

Alassane-Kpembi I., Puel O., Oswald I.P. 2015. 'Toxicological interactions between the mycotoxins deoxynivalenol, nivalenol and their acetylated derivatives in intestinal epithelial cells', *Arch Toxicol*., 8:1337:1346. doi: 10.1007/s00204-014-1309-4.

Alassane-Kpembi I., Gerez J.R., Cossalter A.M., Neves M., Laffitte J., Naylies C., Lippi Y., Kolf-Clauw M., Bracarense AP.F.L., Pinton P., Oswald I.P. 2017a. 'Intestinal toxicity of the type B trichothecene mycotoxin fusarenon-X: whole transcriptome profiling reveals new signaling pathways', *Sci. Rep.* 7:7530. doi: 10.1038/s41598-017-07155-2.

Alassane-Kpembi I., Puel O., Pinton P., Cossalter A.M., Chou T.C., Oswald I.P. 2017b. 'Co-exposure to low doses of the food contaminants Deoxynivalenol and Nivalenol has a synergistic inflammatory effect on intestinal explants', *Arch Toxicol*. 91: 2677-87. doi: 10.1007/s00204-016-1902-9.

Anastassiadou M., Arena M., Auteri D., Brancato A., Bura L., Carrasco Cabrera L., Chaideftou E., Chiusolo A., Crivellente F., De Lentdecker C. *et al.* 2020. 'Peer review of the pesticide risk assessment of the active substance captan', *EFSA Journal*, 18:6230. doi :10.2903/j.efsa.2020.6230.

Aupanun S., Poapolathep S., Phuektes P., Giorgi M., Zhang Z., Oswald I.P, Poapolathep A. 2019. 'Individual and combined mycotoxins deoxynivalenol, nivalenol, and fusarenon-X induced apoptosis in lymphoid tissues of mice after oral exposure', *Toxicon*., 165:83-94. doi: 10.1016/j.toxicon.2019.04.017.

Bastide N.M., Pierre F.H., Corpet D.E. 2011. 'Heme iron from meat and risk of colorectal cancer: a meta-analysis and a review of the mechanisms involved', *Cancer Prev. Res. (Phila)*, 4:177-84. doi: 10.1158/1940-6207.CAPR-10-0113.

Basu A.K. 2018. 'DNA Damage, Mutagenesis and Cancer', *Int. J. Mol. Sci*., 19:970. doi: 10.3390/ijms19040970.

Bianco G., Fontanella B., Severino L., Quaroni A., Autore G., Marzocco S. 2012. 'Nivalenol and deoxynivalenol affect rat intestinal epithelial cells: a concentration related study', *PLoS One*, 7:e52051. doi:10.1371/journal.pone.0052051.

Bossuet-Greif N., Vignard J., Taieb F., Mirey G., Dubois D., Petit C., Oswald E., Nougayrède J.P. 2018. 'The Colibactin Genotoxin Generates DNA Interstrand Cross-Links in Infected Cells', *mBio*, 9: e02393. doi:10.1128/mBio.02393-17.

Brooks P.J., Zakhari S. 2014. 'Acetaldehyde and the genome: beyond nuclear DNA adducts and carcinogenesis', *Environ. Mol. Mutagen*., 55:77-91. doi: 10.1002/em.21824.

Chagneau C.V., Payros D., Tang-Fichaux M., Auvray F., Nougayrède J.P., Oswald E. 2022. 'The pks island: a bacterial Swiss army knife?', *Trends Microbiol.* doi: 10.1016/j.tim.2022.05.01.

Chen J., Stubbe J. 2005. 'Bleomycins: towards better therapeutics', *Nat. Rev. Cancer*, 5:102–112. doi:10.1038/nrc1547.

Cundliffe E., Davies J.E. 1977. 'Inhibition of initiation, elongation, and termination of eukaryotic protein synthesis by trichothecene fungal toxins', *Antimicrob Agents Chemother.,* 11:491-9. doi: 10.1128/AAC.11.3.491.

Dani C., Piechaczyk M., Audigier Y., El Sabouty S., Cathala G., Marty L., Fort P., Blanchard J.M., Jeanteur P. 1984. 'Characterization of the transcription products of glyceraldehyde 3-phosphate-dehydrogenase gene in HeLa cells', *Eur J Biochem*. 14:299-304. doi: 10.1111/j.1432-1033.1984.tb08552.x.

Eskola, M., Elliott, C.T., Hajšlov, J., Steiner, D., Krska, R. 2020. 'Towards a dietary-exposome assessment of chemicals in food: an update on the chronic health risks for the European consumer', *Crit. Rev. Food Sci. Nutr*., 60:1890–1911. doi:10.1080/10408398. 2019.1612320.

European Commission. 2008. 'Regulation No 1272/2008 of the European Parliament and of the Council of 16 December 2008 on classification, labelling and packaging of substances and mixtures, amending and repealing Directives 67/548/EEC and 1999 /45/EC and amending Regulation (EC) No 1907/2006'. *Official journal of the European Union*, 354:1-1355.

Fernández-Blanco C., Elmo L., Waldner T., Ruiz M.J. 2018. 'Cytotoxic effects induced by patulin, deoxynivalenol and toxin T2 individually and in combination in hepatic cells (HepG2)', *Food Chem Toxicol*., 120:12-23. doi: 10.1016/j.fct.2018.06.019.

Fernandez-Vidal A., Arnaud L.C., Maumus M., Chevalier M., Mirey G., Salles B., Vignard J., Boutet-Robinet E. 2019. 'Exposure to the Fungicide Captan Induces DNA Base Alterations and Replicative Stress in Mammalian Cells', *Environ. Mol. Mutagen*. 3:286-297. doi: 10.1002/em.22268.

Foroud N.A., Baines D., Gagkaeva T.Y., Thakor N., Badea A., Steiner B., Bürstmayr M., Bürstmayr H. 2019. 'Trichothecenes in Cereal Grains – An Update', *Toxins*, 11:634. doi: 10.3390/toxins11110634.

Garcia G.R., Payros D., Pinton P., Dogi C.A., Laffitte J., Neves M., Gonzalez-Pereyra M.L., Cavaglieri L.R., Oswald I.P. 2018. Intestinal toxicity of deoxynivalenol is limited by *Lactobacillus rhamnosus* RC007 in pig jejunum explants. *Arch Toxicol.* 92: 983-993. doi: 10.1007/s00204-017-2083-x

Garreau de Loubresse N., Prokhorova I., Holtkamp W., Rodnina V., Yusupova G., Yusupov M., 2014. 'Structural basis for the inhibition of the eukaryotic ribosome', *Nature,* 513: 517–522. doi:10.1038/nature13737.

Garofalo M., Payros, D., Oswald E., Nougayrède J.P., Oswald I.P. 2022. 'The foodborne contaminant deoxynivalenol exacerbates DNA damage caused by a broad spectrum of genotoxic agents', *STOTEN*, 820:153280. doi:10.1016/j.scitotenv.2022.153280.

Gottschalk C., Bauer J., Meyer K. 2008. 'Detection of satratoxin g and h in indoor air from a water-damaged building', *Mycopathol.*, 166:103-7. doi: 10.1007/s11046-008-9126-z.

Henrich C.J. 2016. 'A Microplate-Based Nonradioactive Protein Synthesis Assay: Application to TRAIL Sensitization by Protein Synthesis Inhibitors', *PloS One*, 11: e0165192. doi:10.1371/journal.pone.0165192.

Huybrechts K., Claeys L., Ferrari P., Altieri A., Arcella D., Papadimitriou C., Casagrande C., Nicolas G., Biessy C., Zavadil J., Gunter M., De Saeger S., De Boevre M. 2019. 'Impact of chronic multi-mycotoxin dietary exposure on colorectal and liver cancer risk in Europe', *World Mycotoxin Forum - Book of Abstracts*, p. 70.

International Agency for Research on Cancer (IARC) Working Group on the Evaluation of Carcinogenic Risks to Humans. 2017. 'Some Organophosphate Insecticides and Herbicides', Lyon (FR), vol. 112. Bookshelf ID: NBK436774.

Jaiswal M., Laurosso, N.F., Burgart L.J. 2000. 'Inflammatory Cytokines Induce DNA damage and Inhibit DNA repair in Cholangiocarcinoma Cells by a Nitric Oxide-dependent Mechanism', *Cancer Res*., 60:184-190.

Johnson J.R., Johnston B., Kuskowski M.A., Nougayrede, J.P., Oswald E. 2008. 'Molecular epidemiology and phylogenetic distribution of the Escherichia coli pks genomic island', *J. Clin. Microbiol*. 46: 3906–3911. doi: 10.1128/JCM.00949-08

Khoshal A.K., Novak B., Martin P.G.P., Jenkins T., Neves M., Schatzmayr G., Oswald I.P., Pinton P. 2019. 'Co-occurrence of DON and Emerging Mycotoxins in Worldwide Finished Pig Feed and Their Combined Toxicity in Intestinal Cells', *Toxins (Basel)*, 12:727. doi: 10.3390/toxins11120727.

Knutsen H.K., Alexander, J., Barregard, L., Bignami, M., Bruschweiler, B., Ceccatelli, S., Cottrill, B., Dinovi, M., Grasl-Kraupp, B., Hogstrand, C. *et al*. 2017a. 'Risks to human and animal health related to the presence of deoxynivalenol and its acetylated and modified forms in food and feed', *EFSA Journal*, 15: e04718. doi: 10.2903/j.efsa.2017.4718.

Knutsen H.K., Barregard L., Bignami M., Bruschweiler B., Ceccatelli S., Cottrill B., Dinovi M., Edler L., Grasl-Kraupp B., Hogstrand C. *et al*. 2017b. 'Appropriateness to set a group health based guidance value for nivalenol and its modified forms', EFSA Journal, 15:4751. doi: 10.2903/j.efsa.2017.4751.

Knutsen H.K., Barregard L., Bignami M., Bruschweiler B., Ceccatelli S., Cottrill B., Dinovi M., Edler L., Grasl-Kraupp B., Hoogenboom L. *et al*. 2017c. 'Appropriateness to set a group health based guidance value for T2 and HT2 toxin and its modified forms', *EFSA Journal*, 15: 4655. doi: 10.2903/j.efsa.2017.4655.

Knutsen H.K, Alexander J., Barregard L., Bignami M, Bruschweiler B, Ceccatelli S., Cottril B, Dinovi M, Grasl-Kraupp B, Hogstrand C. *et al*. 2018. Risk to human and animal health related to the presence of 4,15- diacetoxyscirpenol in food and feed', *EFSA Journal*, 16:8. doi:10.2903/j.efsa.2018.5367.

Luongo D., Severino L., Bergamo P., D'Arienzo R., Rossi M. 2010. 'Trichothecenes NIV and DON modulate the maturation of murine dendritic cells', *Toxicon*., 55:73-80. doi: 10.1016/j.toxicon.2009.06.039.

Maresca M. 2013. 'From the gut to the brain: journey and pathophysiological effects of the food-associated trichothecene mycotoxin deoxynivalenol', *Toxins (Basel)*, 23:784-820. doi: 10.3390/toxins5040784.

Martin P., Marcq I., Magistro G., Penary M., Garcie C. Payros D., Boury M., Olier M., Nougayrède J.P., Audebert M., Chalut C., Schubert S., Oswald, E. 2013. 'Interplay between Siderophores and Colibactin Genotoxin Biosynthetic Pathways in *Escherichia coli*', *PLoS Pathog*., 9:e1003437. doi:10.1371/journal.ppat.1003437.

Moon Y., Uzarski R., Pestka J.J. 2003. 'Relationship of trichothecene structure to COX-2 induction in the macrophage: selective action of type B (8-keto) trichothecenes', *J. Toxicol., Environ Health A*. 66:1967-83. doi: 10.1080/713853950.

Nougayrède J.P., Homburg S., Taieb F., Boury M., Brzuszkiewicz E., Gottschalk G., Buchrieser C., Hacker J., Dobrindt U., Oswald E. 2006. '*Escherichia coli* Induces DNA Double-Strand Breaks in Eukaryotic Cells', *Science*, 313: 848–851. doi:10.1126/science.1127059.

475 Payros D., Secher T., Boury M., Brehin C., Ménard S., Salvador-Cartier C., Cuevas-
476 Ramos G., Watrin C., Marcq I., Nougayrède J.P., *et al.* 2014. 'Maternally acquired genotoxic
477 *Escherichia coli* alters offspring's intestinal homeostasis', *Gut Microbes*, 5: 313–512.
478 doi:10.4161/gmic.28932.
479 Payros D., Alassane-Kpembi I., Pierron A., Loiseau N., Pinton P., Oswald I.P. 2016.
480 'Toxicology of deoxynivalenol and its acetylated and modified forms', *Arch. Toxicol.*, 90:
481 2931–2957. doi:10.1007/s00204-016-1826-4.
482 Payros D., Dobrindt U., Martin P., Secher T., Bracarense A.P.F.L., Boury M., Laffitte
483 J., Pinton P., Oswald E., Oswald I.P. 2017. 'The Food Contaminant Deoxynivalenol
484 Exacerbates the Genotoxicity of Gut Microbiota', *mBio*, 8: e007-17. doi:10.1128/mBio.00007-
485 17.
486 Payros D., Garofalo, M., Pierron A., Soler-Vasco L., Al-Ayoubi C., Maruo, V.M.,
487 Alassane- Kpembi I., Pinton P., Oswald, I.P. 2021a. 'Mycotoxins in human food: a challenge
488 for research'. *Cah. Nutr. Diet.,* 56: 170–183. doi:10.1016/j.cnd.2021.02.001.
489 Payros D., Alassane-Kpembi I., Laffitte J., Lencina C., Neves M., Bracarense A.P.,
490 Pinton P., Ménard S., Oswald I.P. 2021b. 'Dietary Exposure to the Food Contaminant
491 Deoxynivalenol Triggers Colonic Breakdown by Activating the Mitochondrial and the Death
492 Receptor Pathways'. *Mol. Nutr. Food. Res.* 65:e2100191. doi: 10.1002/mnfr.202100191.
493 Pestka, J.J. 2010. 'Deoxynivalenol-Induced Proinflammatory Gene Expression:
494 Mechanisms and Pathological Sequelae', *Toxins*, 2:1300–1317. doi:10.3390/toxins2061300.
495 Pierron A., Neves M., Puel S., Lippi Y., Soler L., Miller J.D., Oswald I.P. 2022.
496 'Intestinal toxicity of the new type A trichothecenes, NX and 3ANX', *Chemosphere.* 288:
497 132415. doi:10.1016/j.chemosphere.2021.132415.
498 Pinton P. and Oswald I.P. 2014. 'Effect of Deoxynivalenol and Other Type B
499 Trichothecenes on the Intestine: A Review', *Toxins*, 6: 1615-1643. doi:
500 10.3390/toxins6051615.
501 Polak-Śliwińska M., Paszczyk B. 2021. 'Trichothecenes in Food and Feed, Relevance
502 to Human and Animal Health and Methods of Detection: A Systematic Review', *Molecules*,
503 26:454. doi:10.3390/molecules26020454.
504 Presutti R., Harris S.A., Kachuri L., Spinelli J.J., Pahwa M., Blair A., Zahm S.H., Cantor
505 K.P., Weisenburger D.D, Pahwa P. et al. 2016. 'Pesticide exposures and the risk of multiple
506 myeloma in men: An analysis of the North American Pooled Project', *Int. J. Cancer*, 139:1703-
507 1714. doi: 10.1002/ijc.30218.

Putze J., Hennequin C., Nougayrède J.P., Zhang W., Homburg S., Karch H., Bringer M.A., Fayolle C., Carniel E., Rabsch W., Oelschlaeger T.A., Oswald E., Forestier C., Hacker J, Dobrindt U. 2009. 'Genetic structure and distribution of the colibactin genomic island among members of the family *Enterobacteriaceae*', *Infect Immun.,* 77:4696-703. doi: 10.1128/IAI.00522-09.

Rogakou E.P., Pilch D.R., Orr A.H., Ivanova V.S., Bonner W.M. 1998. 'DNA Double-stranded Breaks Induce Histone H2AX Phosphorylation on Serine 139', *J. Biol. Chem.*, 273: 5858–5868. doi:10.1074/jbc.273.10.5858.

Schothorst R.C. and van Egmond H.P. 2003. 'Report from SCOOP task 3.2.10: collection of occurrence data of *Fusarium* toxins in food and assessment of dietary intake by the population of EU member states. Subtask: trichothecenes', *Toxicol. Lett*., 153:133-43. doi: 10.1016/j.toxlet.2004.04.045.

Seeboth J., Solinhac R., Oswald I.P., Guzylack-Piriou L. 2012. 'The fungal T-2 toxin alters the activation of primary macrophages induced by TLR-agonists resulting in a decrease of the inflammatory response in pigs', *Vet Res.* 43:35. doi: 10.1186/1297-9716-43-35.

Shinde R., Shiragave P., Lakade A., Thorat P., Banerjee K. 2019. 'Multi-residue analysis of captan, captafol, folpet, and iprodione in cereals using liquid chromatography with tandem mass spectrometry', *Food Addit. Contam. Part A Chem. Anal. Control Expo. Risk Assess*., 36:1688-1695. doi: 10.1080/19440049.2019.1662953.

Soler L., Miller I., Terciolo C., Hummel K., Nöbauer K., Neves M., Oswald I.P. 2022. 'Exposure of intestinal explants to NX, but not to DON, enriches the secretome in mitochondrial proteins', *Arch. Toxicol.* doi: 10.1007/s00204-022-03318-x.

Spriggs K.A., Bushell M. and Willis A.E. 2010. 'Translational Regulation of Gene Expression during Conditions of Cell Stress', *Molecular Cell*, 40: 228–237. doi:10.1016/j.molcel.2010.09.028.

Steinkellner H., Binaglia M., Dall'Asta C., Gutleb A.C., Metzler M., Oswald I.P., Parent-Massin D., Alexander J. 2019. Combined hazard assessment of mycotoxins and their modified forms applying relative potency factors: Zearalenone and T2/HT2 toxin. *Food Chem Toxicol.* 131:110599. doi: 10.1016/j.fct.2019.110599.

Taieb F., Petit C., Nougayrède J.P., Oswald E. 2016. 'The Enterobacterial Genotoxins: Cytolethal Distending Toxin and Colibactin', *EcoSal Plus*, 7:1. doi: 10.1128/ecosalplus.ESP-0008-2016. PMID: 27419387.

Tani N., Dohi Y., Onji Y., Yonemasu K. 1995. 'Antiviral activity of trichothecene mycotoxins (deoxynivalenol, fusarenon-X, and nivalenol) against herpes simplex virus types 1

542 and 2', *Microbiol Immunol*., 39: 635-7. doi: 10.1111/j.1348-0421.1995.tb02254.x.
543 Tenaillon O. Skurnik D., Picard B., Denamur E. 2010. 'The population genetics of
544 commensal *Escherichia coli*', *Nat. Rev. Microbiol.*, 8:207–217. doi:10.1038/nrmicro2298.
545 Terciolo C., Maresca M., Pinton P., Oswald I.P. 2018. 'Review article: Role of satiety
546 hormones in anorexia induction by Trichothecene mycotoxins', *Food Chem. Toxicol.*, 121:701–
547 714. doi:10.1016/j.fct.2018.09.034.
548 Theumer M.G., Henneb Y., Khoury L., Snini S.P., Tadrist S., Canlet C., Puel O., Oswald
549 I.P., Audebert M. 2018. 'Genotoxicity of aflatoxins and their precursors in human cells',
550 *Toxicol Lett.,* 287:100-107. doi: 10.1016/j.toxlet.2018.02.007.
551 Tronnet S. and Oswald, E. 2018. 'Quantification of Colibactin-associated Genotoxicity
552 in HeLa Cells by In Cell Western (ICW) Using γ-H2AX as a Marker', *Bio Protoc.*, 8:e2771.
553 doi:10.21769/BioProtoc.2771.
554 Van Der Fels-Klerx H.J., Liu C., Battilani P. 2016. 'Modelling climate change impacts
555 on mycotoxin contamination', *World Mycotoxins J.,* 5:717 -726. doi:10.3920/WMJ2016.2066
556 Varga E., Wiesenberger G., Hametner C., Ward T.J., Dong Y., Schöfbeck D.,
557 McCormick S., Broz K., Stückler R., Schuhmacher R. *et al*. 2015. 'New tricks of an old enemy:
558 isolates of *Fusarium graminearum* produce a type A trichothecene mycotoxin', *Environ.*
559 *Microbiol.* 17:2588-600. doi: 10.1111/1462-2920.12718.
560 Varga E., Wiesenberger G., Woelflingseder L., Twaruschek K., Hametner C.,
561 Vaclaviková M., Malachová A., Marko D., Berthiller F., Adam G. 2018. 'Less-toxic
562 rearrangement products of NX-toxins are formed during storage and food processing', *Toxicol.*
563 *Lett*., 284:205-212. doi: 10.1016/j.toxlet.2017.12.016.
564 Wang W. Zhu Y., Abraham N., Li X.Z., Kimber M., Zhou T. 2021. 'The Ribosome-
565 Binding Mode of Trichothecene Mycotoxins Rationalizes Their Structure—Activity
566 Relationships', *Int. J. Mol. Sci.*, 22:1604. doi:10.3390/ijms22041604.
567 Weaver G.A., Kurtz H.J., Bates F.Y., Mirocha C.J., Behrens J.C., Hagler W.M. 1981.
568 'Diacetoxyscirpenol toxicity in pigs'. *Res. Vet. Sci*., 31:131-5. doi: 10.1016/S0034
569 5288(18)32480-9.
570 Wu Q., Dohnal V., Kuca K., Yuan Z. 2013. 'Trichothecenes: Structure-toxic activity
571 relationships'*, Curr. Drug Metab*., 14:641–660. doi: 10.2174/1389200211314060002.
572 Wyatt R.D., Hamilton P.B., Burmeister, H.R. 1973. 'The Effects of T-2 Toxin in Broiler
573 Chickens', *Poultry Science*, 52:1853-1859. doi:10.3382/ps.0521853.

Yang Y., Gharaibeh R.Z., Newsome R.C., Jobin C. 2020. 'Amending microbiota by targeting intestinal inflammation with TNF blockade attenuates development of colorectal cancer', *Nat Cancer*., 7:723-734. doi: 10.1038/s43018-020-0078-7.

Zhou H.R., He K., Landgraf J., Pan X., Pestka J.J. 2014. 'Direct Activation of Ribosome-Associated Double-Stranded RNA-Dependent Protein Kinase (PKR) by Deoxynivalenol, Anisomycin and Ricin: A New Model for Ribotoxic Stress Response Induction', *Toxins*, 6: 3406–3425. doi:10.3390/toxins6123406.

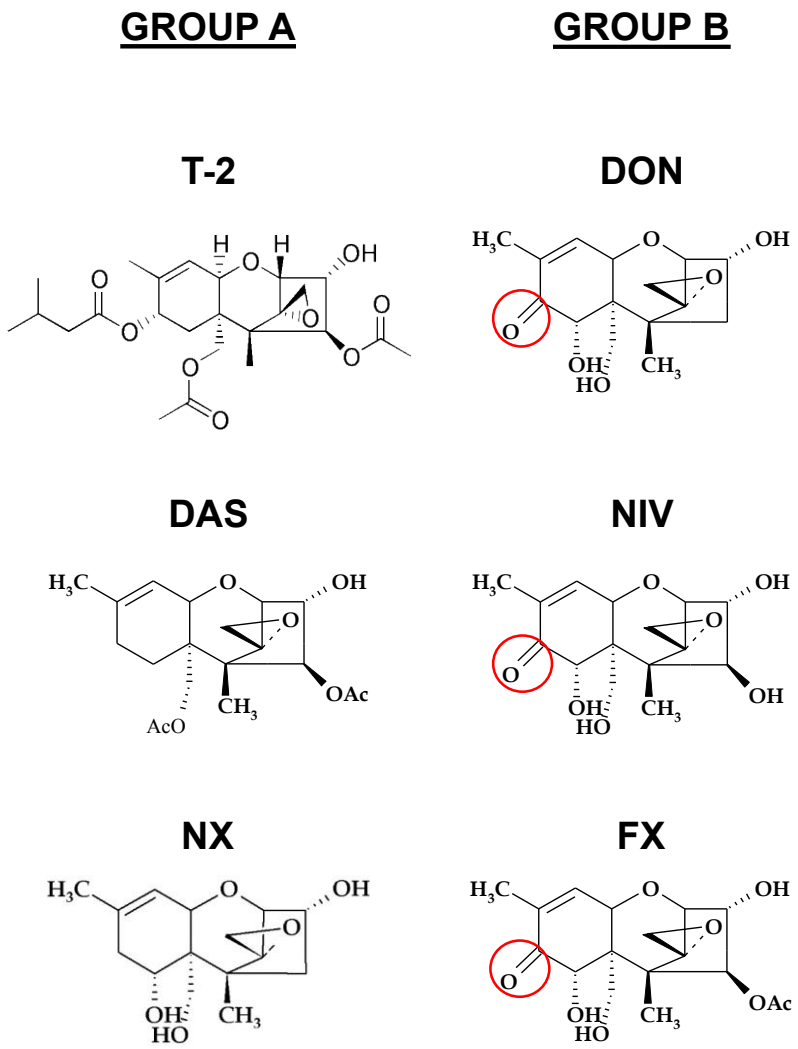

Figure 1: Chemical structures of trichothecenes. Dietary TCTs are classified in two main groups. Group A TCTs include T-2 toxin (T-2), diacetoxyscirpenol (DAS), and NX. Groupe B TCTs include deoxynivalenol (DON), nivalenol (NIV), and fusarenon-X (FX). Group A TCTs can be distinguished from group B TCTs by the presence of a C_8 keto-oxygen (circled in red).

A

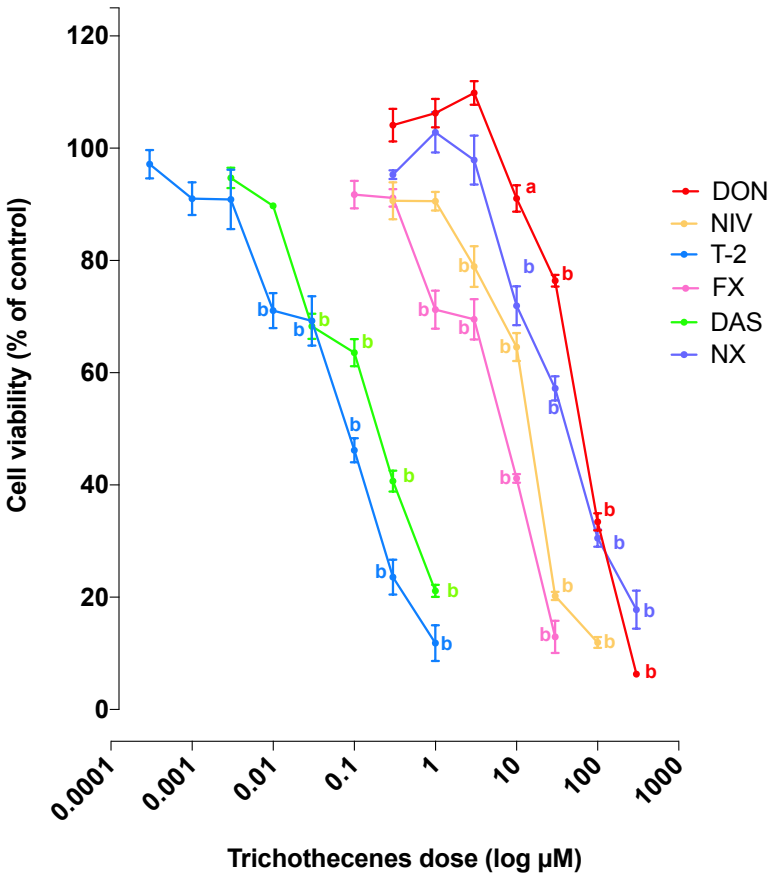

B

	IC_{20}
T-2	18.1 nM *(10.6 - 30.7 nM)*
DAS	31.1 nM *(19.6 - 49.4 nM)*
FX	2.8 µM *(1.4 - 6.1 µM)*
NIV	4.2 µM *(2.6 - 6.7 µM)*
NX	10.4 µM *(6.3 - 15.7 µM)*
DON	20.2 µM *(15.4 - 26.7 µM)*

Figure 2: Trichothecenes induce dose-dependent cytotoxicity in cultured intestinal epithelial cells. A: Non-transformed rat intestinal epithelial IEC-6 cells were treated for 24 h with various concentrations of TCTs and then viability was assessed by measuring ATP levels. Data are expressed as mean ± SEM (3 to 6 independent experiments). P-values were calculated using one-way ANOVA with Bonferroni's multiple comparison, a: $p<0.01$; b: $p<0.0001$: B: Concentrations that inhibited cell viability by 20% (IC_{20}) for each trichothecene were calculated using the data presented in panel A. 95% confidence intervals are shown in italics.

A

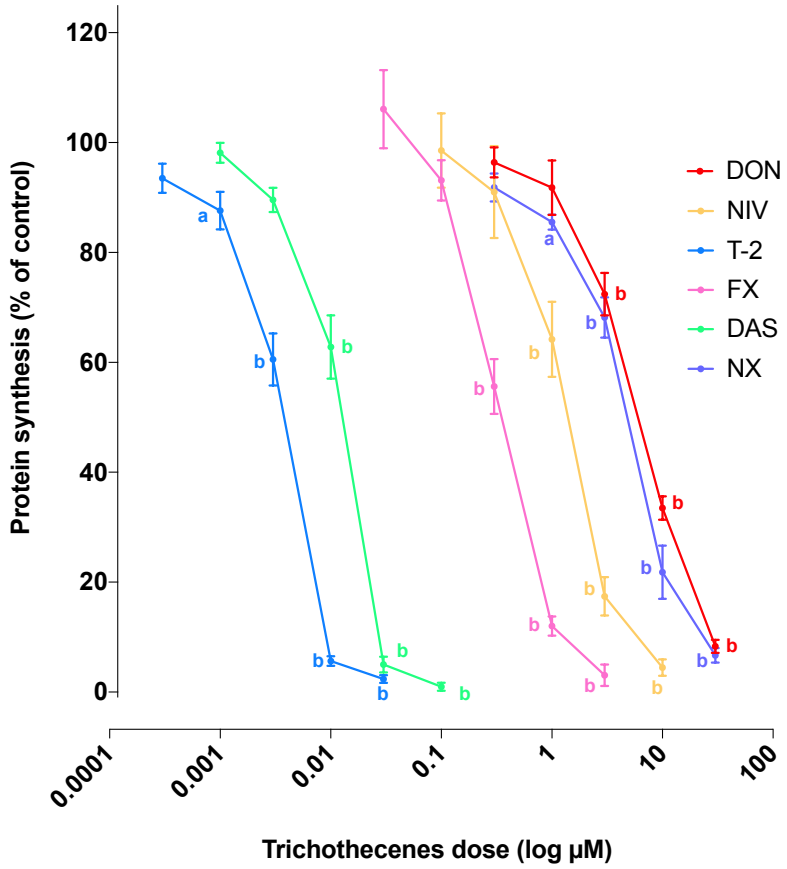

B

	20% PSI level
T-2	1.9 nM *(1.6 - 2.3 nM)*
DAS	6 nM *(5 - 7 nM)*
FX	0.15 µM *(0.12 - 0.19 µM)*
NIV	0.6 µM *(0.4 - 0.9 µM)*
NX	2.5 µM *(2.0 - 3.1 µM)*
DON	2.9 µM *(2.2 - 3.9 µM)*

Figure 3: Trichothecenes induce dose-dependent ribotoxicity in cultured intestinal epithelial cells. A: IEC-6 cells were treated for 4 h with different concentrations of TCTs and then the cells were treated for 30 min with puromycin, a protein translation marker. Incorporation of puromycin into newly synthesized peptides was quantified with an anti-puromycin antibody by In-Cell-Western. All the data are expressed as mean ± SEM (4 independent experiments). Values that are significantly different compared to the vehicle control are indicated a: $p<0.01$; b: $p<0.0001$: B: Concentrations that inhibited the protein synthesis by 20% (20% PSI) were calculated using the data presented in panel A. 95% confidence intervals are shown in italics.

A

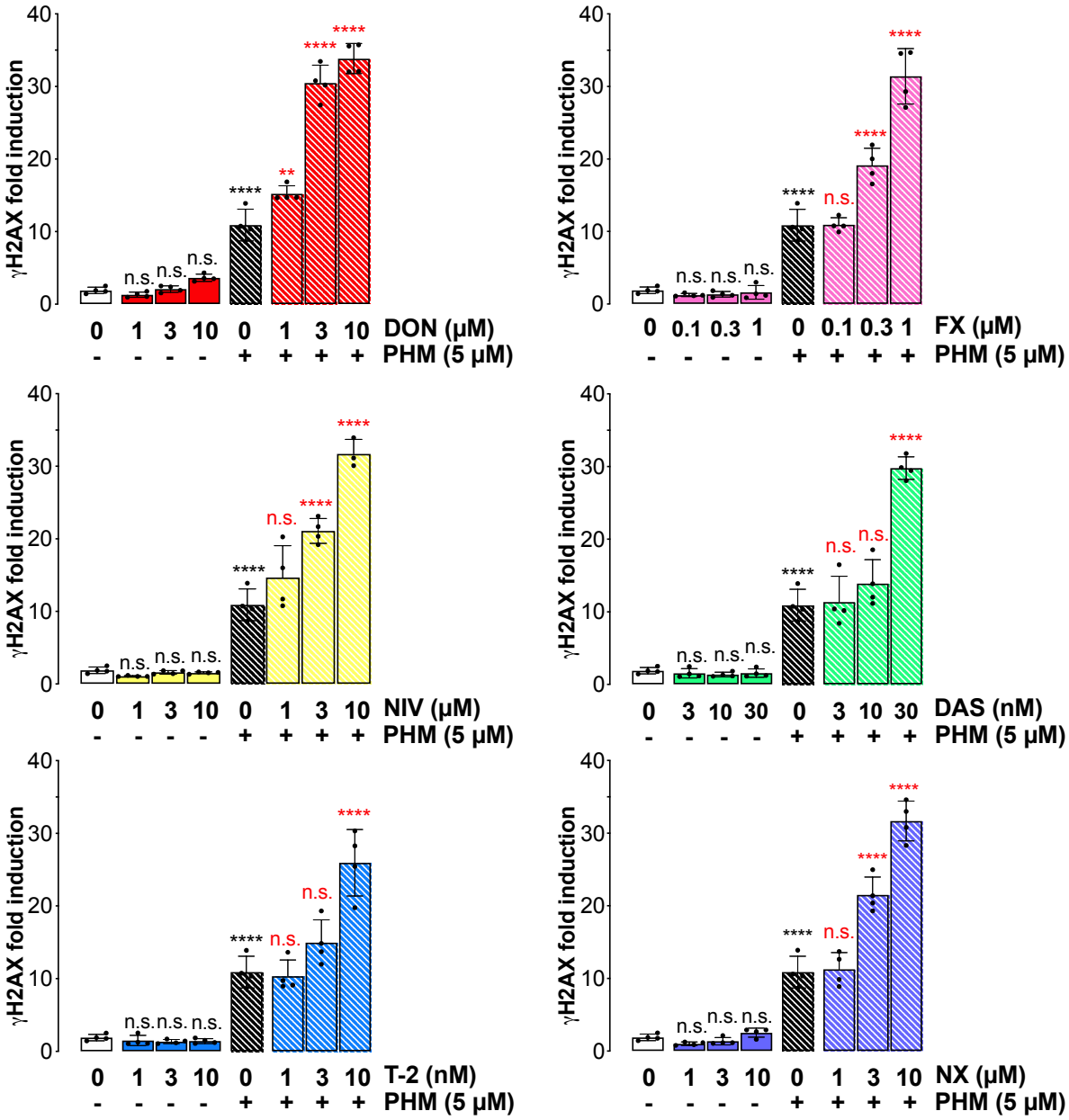

B

No effect dose					
T-2	**DAS**	**FX**	**NIV**	**DON**	**NX**
3 nM	10 nM	0.1 μM	1 μM	< 1 μM	1 μM

Figure 4: Trichothecenes exacerbate the genotoxicity induced by the DNA-damaging drug phleomycin in a dose-dependent manner. A: IEC-6 cells were co-treated for 4 h with 5 µM phleomycin (PHM) and increasing doses of DON (red), NIV (yellow), T-2 (blue), FX (pink), DAS (green), or NX (purple). Then, DNA damage was measured by quantification of H2AX phosphorylation by In-Cell-Western. All data are expressed as mean ± SEM (4 independent experiments). P-values were calculated using a one-way ANOVA with Bonferroni's multiple comparison. Values that are significantly different compared to vehicle are indicated by black asterisks, and values that are significantly different from infected cells without TCT are indicated by red asterisks. *:$p<0.1$; **: $p< 0.01$; ***: $p<0.001$, ****: $p< 0.0001$, n.s. : not significant. B: No exacerbation doses for each TCT were defined from data in panel A.

A

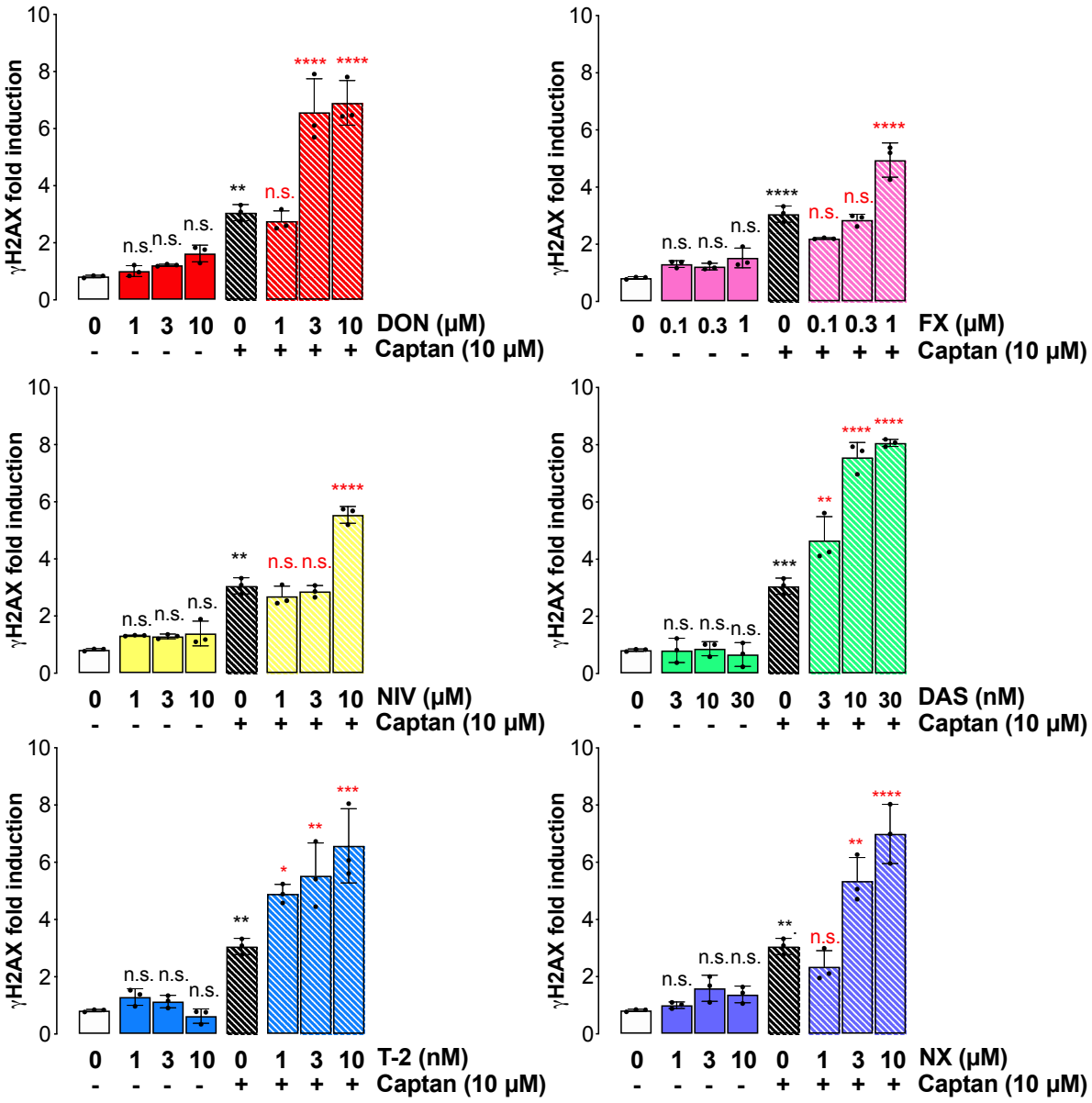

B

No effect dose					
T-2	**DAS**	**FX**	**NIV**	**DON**	**NX**
< 1 nM	< 3 nM	0.3 µM	3 µM	1 µM	1 µM

Figure 5: Trichothecenes exacerbate the genotoxicity induced by the fungicide captan in a dose-dependent manner. A: IEC-6 cells were co-treated for 4 h with 10 µM captan and increasing doses of DON (red), NIV (yellow), T-2 (blue), FX (pink), DAS (green), or NX (purple). Then, DNA damage was measured by quantification of H2AX phosphorylation by In-Cell-Western. All data are expressed as mean ± SEM (3 independent experiments). P-values were calculated using one-way ANOVA with Bonferroni's multiple comparison. Values that are significantly different compared to vehicle are indicated by black asterisks, and values that are significantly different from infected cells without TCT are indicated by red asterisks. *:$p<0.1$; **: $p< 0.01$; ***: $p<0.001$, ****: $p< 0.0001$, n.s.: not significant. B: No exacerbation dose for each TCT was defined from data in panel A.

A

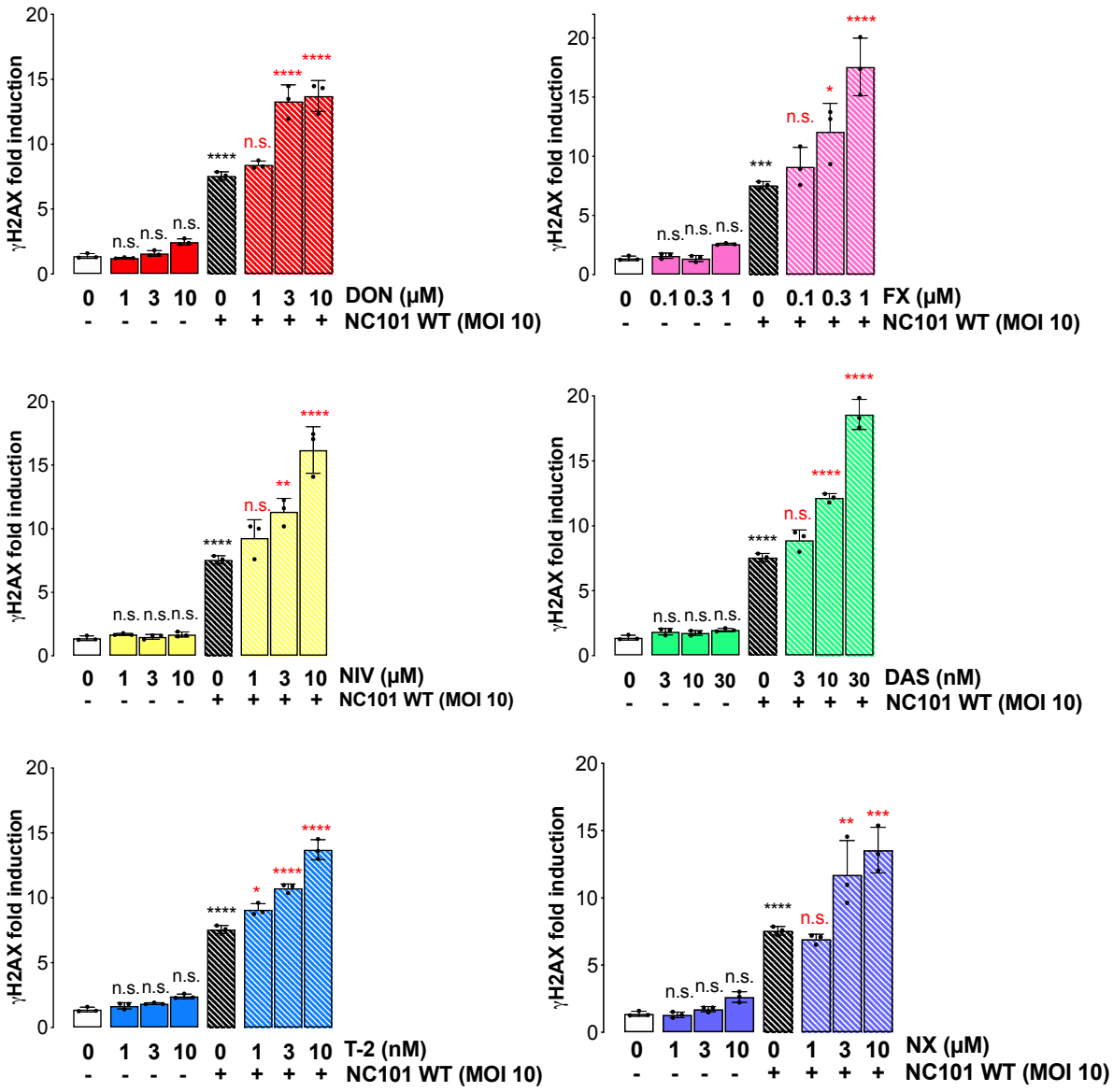

B

No effect dose					
T-2	**DAS**	**FX**	**NIV**	**DON**	**NX**
< 1 nM	3 nM	0.1 μM	0.3 μM	1 μM	1 μM

Figure 6: Trichothecenes exacerbate the genotoxicity induced by the bacterial genotoxin colibactin in a dose-dependent manner. A: IEC-6 cells were infected 4 h with live colibactin-producing *E. coli* strain NC101 (multiplicity of infection of 10 bacteria per cell) with increasing doses of DON (red), NIV (yellow), T-2 (blue), FX (pink), DAS (green), or NX (purple). Cells were washed to remove bacteria and further incubated with the TCTs for 4 h. Then, DNA damage was measured by quantification of H2AX phosphorylation by In-Cell-Western. All data are expressed as mean ± SEM (3 independent experiments). P-values were calculated using one-way ANOVA with Bonferroni's multiple comparison. Values that are significantly different compared to vehicle are indicated by black asterisks, and values that are significantly different from infected cells without TCT are indicated by red asterisks. *: $p<0.1$; **: $p< 0.01$; ***: $p<0.001$, ****: $p< 0.0001$, n.s.: not significant. B: No exacerbation doses for each TCT were defined from data shown in figure 6A.

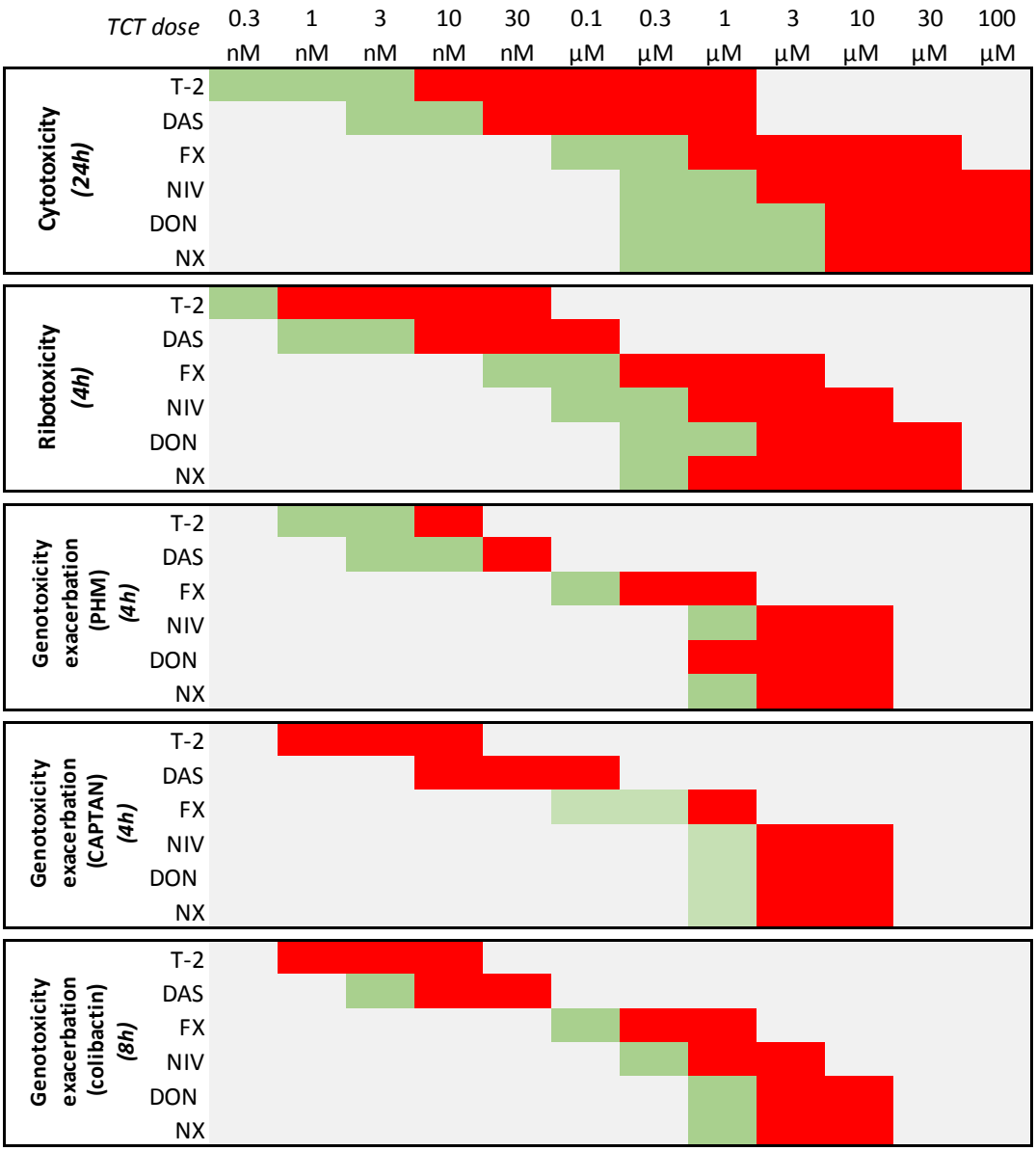

Table 1: Trichothecenes classification for cytotoxicity, ribotoxicity, and capacity to exacerbate the genotoxicity. Green boxes: doses inducing no significant cytotoxicity, ribotoxicy or genotoxicity exacerbation. Red boxes: doses inducing significant cytotoxicity, ribotoxicity or genotoxicity exacerbation.

HIGHLIGHTS

- A novel effect of trichothecenes (TCTs) has been identified
- TCTs exacerbate genotoxicity
- Six type A or type B TCTs display this effect
- This effect is observed with a drug, a pesticide, and a toxin produced by microbiota
- For genotoxicity exacerbation, TCTs are classified: T-2>DAS>FX>NIV≥DON≥NX

GRAPHICAL ABSTRACT

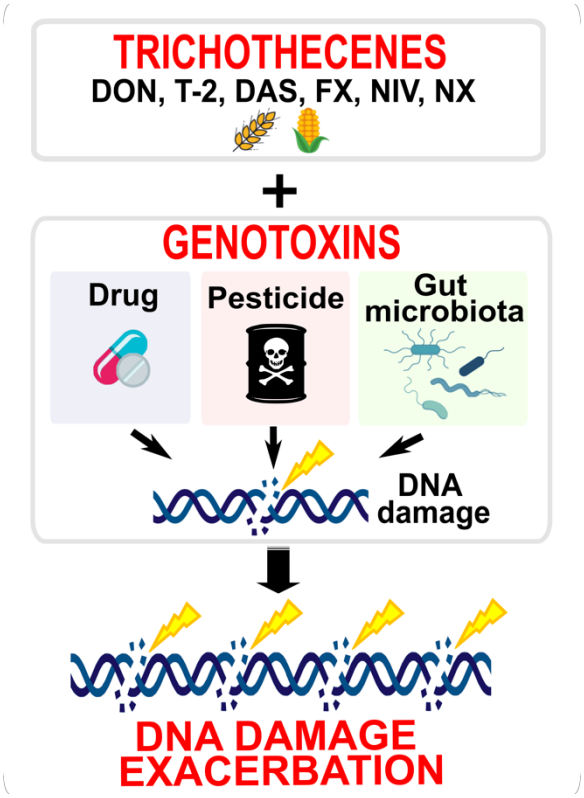

Supplementary material for

"A novel toxic effect of trichothecenes: the exacerbation of genotoxicity"

Marion Garofalo[a,b], Delphine Payros[a,b], Marie Penary[b], Eric Oswald[b,c], Jean-Philippe Nougayrède[b*], Isabelle P. Oswald[a*].

[a]Toxalim (Research Centre in Food Toxicology), Université de Toulouse, INRAE, ENVT, INP-Purpan, UPS, Toulouse, France

[b]IRSD, Université de Toulouse, INSERM, INRAE, ENVT, UPS, Toulouse, France

[c]CHU Toulouse, Hôpital Purpan, Service de Bactériologie-Hygiène, Toulouse, France

*Corresponding authors: isabelle.oswald@inrae.fr; jean-philippe.nougayrede@inrae.fr

Keywords: trichothecenes; genotoxins; colibactin; DNA damage.

Supplementary methods 1:

***In vitro* crosslinking assay and bacterial load analysis.** To examine colibactin production by the bacteria, a DNA crosslinking assay was performed as previously described (Bossuet-Greif *et al.*, 2018). Briefly, 400 ng linear DNA was exposed to 1.5×10^6 bacteria in 100 µl infection medium in the presence of TCTs or DMSO vehicle. After 4 h at 37°C, bacteria were pelleted, plated on LB agar plates, and enumerated. The DNA was purified from the culture supernatant using the Qiagen QIAquick PCR kit (Qiagen, Hilden, Germany). Purified DNA was loaded on a denaturing agarose gel (pH 8) and electrophoresis was carried for 45 min at 25V followed by 2 h 30 min at 50V. After gel neutralization, DNA was stained with Gel Red (Biotium, San Francisco, USA) and visualized in a Bio-Rad Chemidoc XRS system. The percentage of crosslinked DNA was quantified by using the FIJI software (https://imagej.net/Fiji).

DNA quantification (% of control cells)					
	No genotoxin ***(4h)***	**No genotoxin** ***(8h)***	**Phleomycin (5 µM)** ***(4h)***	**Captan (10 µM)** ***(4h)***	**NC101 WT (MOI 10)** ***(8h)***
Control (vehicle)	100	100	98.8 ± 1.6	90.1 ± 1.3	105.1 ± 2.8
DON (10 µM)	83.7 ± 5.8	87.6 ± 6.9	82.4 ± 13.2	99.8 ± 12.5	91.6 ± 8.5
T-2 (10 nM)	86.2 ± 6.6	95.5 ± 2.0	97.7 ± 17.9	107.6 ± 7.8	112.8 ± 3.7
DAS (30 nM)	92.2 ± 12.8	94.2 ± 6.2	104.1 ± 11.6	108.8 ± 3.04	111.4 ± 3.7
NIV (3 µM)	100.6 ± 5.4	103.9 ± 8.4	100.1 ± 6.2	114.7 ± 4.3	109.8 ± 7.4
FX (1 µM)	101.8 ± 3.4	103.7 ± 1.0	90.5 ± 5.2	107.9 ± 12.0	107.0 ± 2.7
NX (10 µM)	85.9 ± 6.9	97.4 ± 2.4	77.4 ± 6.8	85.5 ± 4.1	79.1 ± 0.9

Table S1: The genotoxicity exacerbation induced by trichothecenes is not associated with cytotoxicity. DNA in the cells was calculated from RedDot2 DNA staining using the In-Cell-Western method. Values were obtained after normalization from untreated cells considered as 100%.

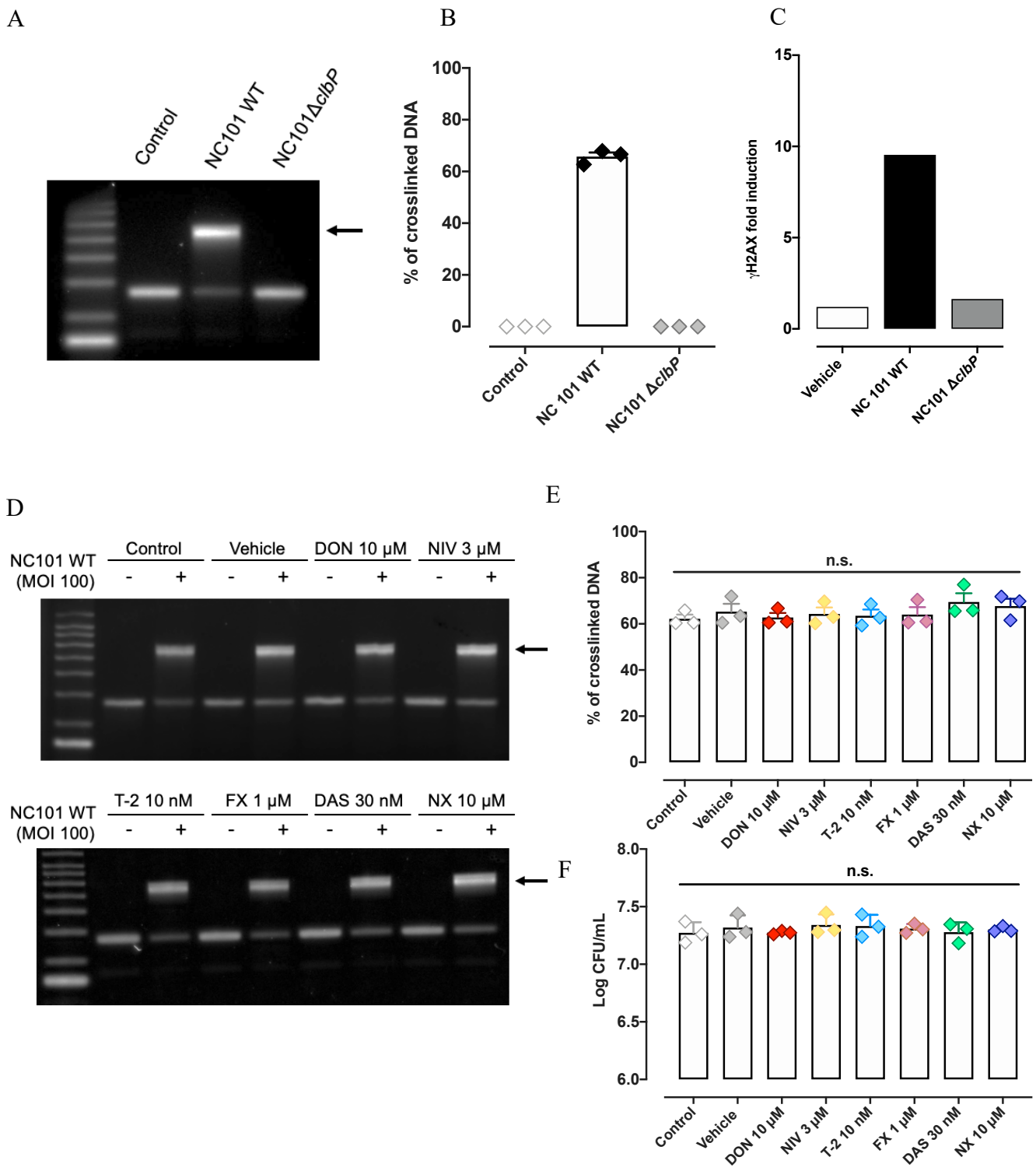

Figure S1: Trichothecenes does not impact colibactin production and bacterial growth. A, B: *E. coli* NC101 WT or Δ*clbP* (MOI 100) were grown for 3.5 h, and then linearized DNA was added and incubated for 30 min. DNA was purified and analysed by denaturing gel electrophoresis, and the percentage of crosslinked DNA (arrow) was quantified by image

analysis. C: Non-transformed rat intestinal epithelial IEC-6 cells were infected for 4 h with the producing-colibactin *E. coli* strain NC101 WT or to the colibactin-deficient strain NC101 Δ*clbP* (MOI 10). Then, H2AX phosphorylation levels were quantified by In-Cell-Western. D, E: colibactin production was measured as in panel A in presence of TCTs. F: after the interaction between bacteria TCT and DNA, the bacteria were counted by serial dilution and plating. After an overnight incubation, Colony Forming Units (CFU) were enumerated. All the data are expressed as mean ± SEM (3 independent experiments). All P-values are calculated using one-way ANOVA with Bonferroni's multiple comparison. n.s: not significant.

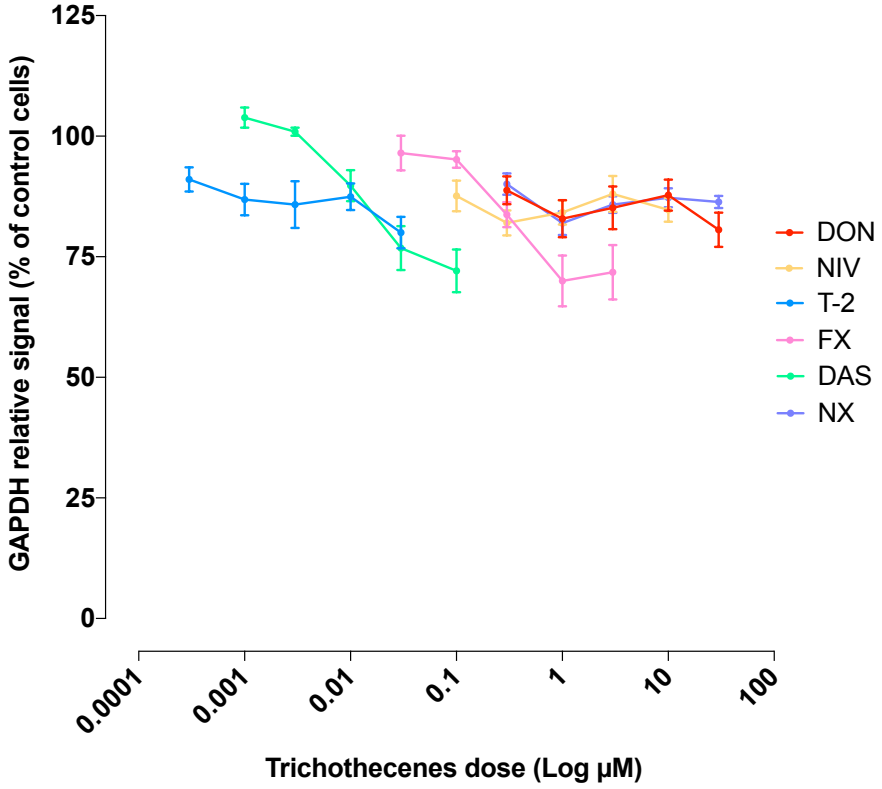

Figure S2: Non-transformed rat intestinal epithelial IEC-6 cells were treated for 4 hours with various concentrations of DON (red), NIV (yellow), T-2 (blue), FX (pink), DAS (green), or NX (purple). GAPDH levels were measured with an anti-GAPDH antibody by In-Cell-Western. All the data are expressed as mean ± SEM (4 independent experiments).